Author Manuscript

Author Manuscript

Author Manuscript

Author Manuscript

HHS Public Access

Author manuscript

Mol Neurobiol. Author manuscript; available in PMC 2016 December 01.

Published in final edited form as:

Mol Neurobiol. 2015 December ; 52(3): 1119–1134. doi:10.1007/s12035-014-8902-7.

Bryostatin-1 Restores Blood Brain Barrier Integrity following Blast-Induced Traumatic Brain Injury

Brandon P. Lucke-Wold,
Department of Neurosurgery, West Virginia University School of Medicine, Morgantown, WV 26506, USA

The Center for Neuroscience, West Virginia University School of Medicine, Morgantown, WV 26506, USA

Aric F. Logsdon,
The Center for Neuroscience, West Virginia University School of Medicine, Morgantown, WV 26506, USA

Department of Basic Pharmaceutical Sciences, West Virginia University School of Pharmacy, Morgantown, WV 26506, USA

Kelly E. Smith,
The Center for Neuroscience, West Virginia University School of Medicine, Morgantown, WV 26506, USA

Department of Basic Pharmaceutical Sciences, West Virginia University School of Pharmacy, Morgantown, WV 26506, USA

Ryan C. Turner,
Department of Neurosurgery, West Virginia University School of Medicine, Morgantown, WV 26506, USA

The Center for Neuroscience, West Virginia University School of Medicine, Morgantown, WV 26506, USA

Daniel L. Alkon,
Blanchette Rockefeller Neurosciences Institute, Morgantown, WV 26506, USA

Zhenjun Tan,
Department of Neurosurgery, West Virginia University School of Medicine, Morgantown, WV 26506, USA

The Center for Neuroscience, West Virginia University School of Medicine, Morgantown, WV 26506, USA

Zachary J. Naser,

Correspondence to: Charles L. Rosen.

Electronic supplementary material The online version of this article (doi:10.1007/s12035-014-8902-7) contains supplementary material, which is available to authorized users.

Conflicts of Interest The authors claim to have no conflicts of interest.

Author Manuscript Author Manuscript Author Manuscript Author Manuscript

Department of Neurosurgery, West Virginia University School of Medicine, Morgantown, WV 26506, USA

The Center for Neuroscience, West Virginia University School of Medicine, Morgantown, WV 26506, USA

Office of Professional Studies in Health Sciences, Drexel University College of Medicine, Philadelphia, PA 19102, USA

Chelsea M. Knotts,
Department of Neurosurgery, West Virginia University School of Medicine, Morgantown, WV 26506, USA

Jason D. Huber, and
The Center for Neuroscience, West Virginia University School of Medicine, Morgantown, WV 26506, USA

Department of Basic Pharmaceutical Sciences, West Virginia University School of Pharmacy, Morgantown, WV 26506, USA

Charles L. Rosen
Department of Neurosurgery, West Virginia University School of Medicine, Morgantown, WV 26506, USA

The Center for Neuroscience, West Virginia University School of Medicine, Morgantown, WV 26506, USA

Department of Neurosurgery, West Virginia University School of Medicine, One Medical Center Drive, Suite 4300, Health Sciences Center, PO Box 9183, Morgantown, WV 26506-9183, USA
crosen@hsc.wvu.edu

Abstract

Recent wars in Iraq and Afghanistan have accounted for an estimated 270,000 blast exposures among military personnel. Blast traumatic brain injury (TBI) is the ‘signature injury’ of modern warfare. Blood brain barrier (BBB) disruption following blast TBI can lead to long-term and diffuse neuroinflammation. In this study, we investigate for the first time the role of bryostatin-1, a specific protein kinase C (PKC) modulator, in ameliorating BBB breakdown. Thirty seven Sprague–Dawley rats were used for this study. We utilized a clinically relevant and validated blast model to expose animals to moderate blast exposure. Groups included: control, single blast exposure, and single blast exposure + bryostatin-1. Bryostatin-1 was administered i.p. 2.5 mg/kg after blast exposure. Evan’s blue, immunohistochemistry, and western blot analysis were performed to assess injury. Evan’s blue binds to albumin and is a marker for BBB disruption. The single blast exposure caused an increase in permeability compared to control (t=4.808, p<0.05), and a reduction back toward control levels when bryostatin-1 was administered (t=5.113, p<0.01). Three important PKC isozymes, PKCα, PKCδ, and PKCε, were co-localized primarily with endothelial cells but not astrocytes. Bryostatin-1 administration reduced toxic PKCα levels back toward control levels (t=4.559, p<0.01) and increased the neuroprotective isozyme PKCε (t=6.102, p<0.01). Bryostatin-1 caused a significant increase in the tight junction proteins VE-cadherin, ZO-1, and occludin through modulation of PKC activity. Bryostatin-1 ultimately

Author Manuscript Author Manuscript Author Manuscript Author Manuscript

decreased BBB breakdown potentially due to modulation of PKC isozymes. Future work will examine the role of bryostatin-1 in preventing chronic neurodegeneration following repetitive neurotrauma.

Keywords

Blood brain barrier; Bryostatin-1; Protein kinase C; Tight junction proteins

Introduction

Each year, 1.7 million Americans experience a traumatic brain injury (TBI) in the USA [1]. Over 70 % of those patients sustain some form of disability following TBI [2]. The mechanisms by which TBI contributes to permanent homeostatic changes within the central nervous system (CNS) remain poorly understood. Recent evidence implicates disruption of the blood brain barrier (BBB) as an important indicator of brain injury [3]. Blast TBI, in particular, contributes to a vascular pressure surge that challenges BBB integrity [4]. Blast TBI also causes significant alterations in ZO-1, occludin, and VE-cadherin, important tight junction proteins [5]. The disruption is not universal across vasculature, however, with scattered lesions spread across the brain at specific microfoci [6]. Oxidative stress from damaged tissue causes increased BBB permeability at these microfoci [7]. The resulting BBB dysfunction contributes to inflammatory cascades and injury expansion [8]. The increase in blast-induced BBB permeability is transient with a return of tight junction function within 3 days, but the subsequent injury response is long-lasting [9].

One possible reason for these long-lasting effects is changes in protein kinase C (PKC) isozyme activity after injury. Some PKC isozymes, PKCα, PKCβ, and PKCε, translocate to the plasma membrane within 3 h after TBI and remain active for days [10–12]. PKCα activity has been linked to neuronal apoptosis following TBI [13] and is closely tied with glutamate receptor signaling [14]. PKCα and PKCδ activity can cause an uncoupling of NMDA receptors from spectrin mediated through sigma-1 receptor activation leading to calcium oscillations [15–17]. The calcium oscillations contribute to mitochondrial dysfunction and cell death [18]. PKCα and PKCδ can also hyperphosphorylate structural proteins such as tau and TBI61 within the hippocampus following injury [19]. Interestingly, PKC activity also decreases cerebral edema following TBI [20]. Three important isozymes play important roles in cerebral vasculature. PKCα regulates ZO-1 and occludin-tight junction proteins [21]. PKCδ activity regulates vessel constriction and vascular tone [22]. PKCε decreases vessel tone and provides neuroprotection [23]. Despite these associations, the role of specific PKC isozymes in BBB disruption following blast TBI has yet to be elucidated.

Although PKC activity has not been well studied in TBI, available evidence suggests that PKC isozymes play an important role in neural injury. An 80% increase in PKC activity was reported 3 h after TBI and contributes to secondary neuronal injury [10]. Compounds that modulate PKC isozymes therefore warrant further investigation. The potent PKC modulator, bryostatin-1, has profound neuroprotective effects in animal models of neural injury. The

Author Manuscript Author Manuscript Author Manuscript Author Manuscript

single study using bryostatin-1 for treatment of mild TBI showed profound protection against learning and memory deficits in mice by increasing the α-secretase, ADAM10 [24]. Although PKC modulation has not been extensively studied in TBI models, in an Alzheimer's disease model it increased PKCε, which facilitated amyloid β plaque degradation by increasing the enzyme neprilysin [25]. It also enhanced gabaergic signaling improving learning and memory through PKCα modulation and decreased synaptic loss [26, 27]. Following ischemic stroke, bryostatin-1 modulated PKCα and PKCε to enhance survival and reduce edema in aged Sprague–Dawley rats [28]. Although Alzheimer's disease and stroke are vastly different than TBI, they do share similar secondary mechanisms of injury, such as PKC and microglia activation, that should be carefully investigated

Herein, we show for the first time that PKC isozymes are increased after blast-induced TBI, and are correlated with acute BBB breakdown and tight junction protein changes. Using our clinically relevant and validated blast model [29], we observed statistically significant acute changes in BBB permeability 6 h after a single blast exposure. Interestingly, the PKC modulator bryostatin-1 reduced BBB permeability, decreased levels of the detrimental PKCα isozyme, and increased the beneficial PKCε isozyme. The mechanism of bryostatin-1's beneficial effects is closely linked to regulation of tight junction proteins through specific modulation of PKC isozymes. Occludin closely interacts with the scaffolding proteins ZO-1 and VE-Cadherin [30], and our data show that bryostatin-1 significantly elevated levels of occludin, VE-Cadherin, and ZO-1. Increasing the levels of tight junction proteins has been shown to help maintain BBB integrity [31]. Modulation of PKC expression may therefore be a promising treatment strategy for preventing BBB disruption following acute neurotrauma.

Materials and Methods

Animals and Treatments

Thirty-seven (37) young adult (300–350 g) male Sprague–Dawley rats (Hilltop Lab Animals, Inc.) were used for this study. Animals were housed in pairs with 12 h:12 h dark to light cycle and food available ad libitum. The Institutional Animal Care and Use Committee of West Virginia University approved all procedures and experiments involving animals. The experiments were performed in accordance with the *Guide for the Care and Use of Laboratory Animals*. Ten (10) animals were used for Evan's Blue (EB) absorbance analysis. Eighteen (18) animals were used for immunohistochemisty (IHC) staining and western blot analysis. Nine (9) animals were used for microvessel isolation and subsequent western blot analysis (Fig. 1). Bryostatin-1 was administered by intraperitoneal injection (2.5 mg/kg) [28], 5 min after blast exposure for all blast + bryostatin-1 groups.

Bryostatin-1 was dissolved in vehicle (10 % ethanol in 0.9 % normal saline). Bryostatin-1 was obtained by Dr. Daniel Alkon from the National Cancer Institute, National Institutes of Health, Bethesda, MD, USA. The dose of bryostatin-1 was selected in accordance with animal protocols and according to a dose response curve showing that bryostatin-1 enters the brain but is maintained well below the maximal tolerated dose [32, 33]. Control animals were anesthetized and injected with vehicle. Bryostatin-1 is a potent modulator of PKC isozymes with selectivity for PKCα and PKCε [34].

Author Manuscript Author Manuscript Author Manuscript Author Manuscript

Blast Exposure

The animal was oriented perpendicular to the blast apparatus, with the driver section placed near the right side of the skull. A polyvinyl chloride shield protected the rest of the body. We utilized a membrane with a 0.005-in. thickness to generate a blast exposure with peak reflected overpressure of ~50 PSI and peak incident overpressure of ~15 PSI (Fig. 1b–c). The exposure produced moderate blast injury as previously characterized. [29]. The primary extent of injury has been localized to the left hemisphere due to coup and counter-coup acceleration/deceleration mechanisms [35]. Briefly, nitrogen gas builds pressure behind a clear polyester film that subsequently ruptures to produce a blast wave. Piezoelectric sensors (Model 102AO5; PCB Piezotronics) were placed in the reflected and incident positions at the exit of the shock tube and data was recorded with a data acquisition board (DAQ 23GF, National Instruments) and sensor signal conditioner (482C Series; PCB Piezotronics). LabView software version 12.0 (National Instruments) was used to reconstruct accurate pressure recording graphs (Fig. 1d). The short driver section generates brief-duration waves comparable to those seen from improvised explosive devices when scaled properly for the rodent size based on principles previously highlighted by Bass and colleagues [36, 37].

Evan's Blue

Groups for Evan's Blue (EB) included control (n=3), single blast (n=4), and single blast + bryostatin-1 (n=3). BBB permeability was assessed 6 h after blast exposure using EB as a tracer molecule. EB binds to albumin, and albumin will only enter the brain if the BBB is compromised. Animals were anesthetized with inhaled 4 % isoflurane (Halocarbon) and maintained with 2 % isoflurane before normal saline containing EB (2 %, 5 mL/kg) (2 %*w/v* in saline) was administered intravenously (femoral vein) 30 min prior to perfusion. The rats were transaortally perfused with normal saline for 10 min. The brains were excised; meninges and ependymal organs removed, hemispheres separated, and left prefrontal cortex sectioned. The prefrontal cortex is one of the brain regions most susceptible to BBB disruption following injury [38]. The left prefrontal cortex samples were then weighed, and homogenized in 1 mL of 50 % trichloroacetic acid (TCA). The resulting suspensions were placed in 0.5 mL aliquots. The aliquots were incubated for 24 h at 37°, and centrifuged at 10,000 × g for 10 min. The supernatant was collected and measured by absorbance spectroscopy at 620 nm for EB determination. Calculations were based on external standard readings (50 μg/mL of EB dissolved in saline with eight serial dilutions). The extravasated dye in brain tissue was expressed as ng EB/mg of brain tissue.

Microvessel Isolation

Rats were anesthetized with 4 % isoflurane, decapitated, and the brain was removed. The brain was placed in 10 mL of MVI Buffer two (6.02 g/L NaCl, 0.35 g/L KCl, 0.37 g/L $CaCl_2$, 0.16 g/L KH_2PO_4, 0.3 g/L $MgSO_4$, and 3.57 g/L HEPES) with protease inhibitor cocktail. The meninges and choroid plexus were removed and the cerebral hemispheres were placed in a glass homogenization tube with 4 mL of MVI Buffer one (6.02 g/L NaCl, 0.35 g/L KCl, 0.37 g/L $CaCl_2$, 0.16 g/L KH_2PO_4, 0.3 g/L $MgSO_4$, 3.57 g/L HEPES, 2.1 g/L $NaHCO_3$, 1.80 g/L Glucose, 0.11 g/L Na Pyruvate, and 10 g/L Dextran (64 K)) and protease inhibitor cocktail. MVIs one and two were pH adjusted to 7.4. With a Teflon pestle, the

Author Manuscript Author Manuscript Author Manuscript Author Manuscript

tissue was homogenized and filtrate placed in a 16-mL tube with 4 mL of 26% dextran. The tubes were centrifuged at 5,800 × *g* for 10 min at 4 °C. The supernatant was aspirated and the pellet was re-suspended in 5 mL of MVI buffer two with protease inhibitor cocktail. The homogenate was filtered through 100 μm filter, and centrifuged at 5,800 × *g* for 5 min at 4 °C. The supernatant was decanted and microvessel pellet saved for western blot analysis.

Western Blot

Western blot analysis was performed similar to work previously published by our laboratory [39]. Briefly, 24 h after blast exposure, animals were anesthetized with 4 % isoflurane, brains were removed by decapitation, and the brains were subsequently sectioned. Groups included control, single blast, and single blast + bryostatin-1. Protein samples from the left prefrontal cortex were dissolved in 0.5 mL hot (85–95 °C)1% sodium docecyl sulfate (SDS), sonicated, and a Bicinchoninic Acid (BCA) protein assay kit (Thermo Fisher Scientific, Rockfield, IL, USA) was used to determine protein concentration. The pre-stained standard SeeBlue® Plus2 (Life Technologies, Carlsbad, CA, USA) was used. 2X Lammeli buffer combined with 30 μg of protein was loaded per well and run on a Bolt® Mini tank system (Life Technologies) with pre-cast Bolt® Bis-Tris Plus 10 % 12-well gels (Life Technologies). PVDF membranes (Bio-Rad, Contra Costa, CA, USA) were soaked in methanol and used for wet transfer (Bio-Rad) at 60 V for 2.5 h. Primary antibodies used were occludin rabbit 1:1,000 (Life Technologies), PKCα, PKCδ, PKCe mouse 1:200 (Santa Cruz Biotechnology, Santa Cruz, CA, USA), and VE-Cadherin rabbit 1:1,000 (Cell Signaling, Danvers, MA, USA). Microvessel isolation tissue was used to detect changes in PKC isozymes. LI-COR secondary antibodies IRDye® 800CW and IRDye® 680RD (LI-COR, Lincoln, NE, USA) were used with an Odyssey fluorescent scanner at wavelengths 800 or 700, intensity 6.0, and 84 resolution with high image quality. Images were analyzed after background subtraction, and normalized to β-actin to give relative overall intensity.

Immunohistochemistry

Experimental groups included control (n=3), single blast (n=3), and single blast + bryostatin-1 (n=3). Rats were anesthetized with 4 % isoflurane and transcardially perfused with 0.9 % saline followed by 4 % paraformaldehyde at 24 h after blast exposure. The rats were decapitated, and brains were removed and stored in 4 % paraformaldehyde until processing. The tissue was sectioned and paraffin embedded. Six-micrometer slices from the left prefrontal cortex were cut with a Leica RM2235 microtome (Leica Microsystems, Wetzlar, Germany) and mounted on slides. Slides were washed in xylene, 100 % EtOH and 95 % EtOH for 5 min each in order to remove the paraffin, followed by rehydration in dH_2O for 5 min. Using 10 % methanol and 10 % H2O2 in Dulbecco's phosphate buffered saline (DPBS), slides were quenched for 15 min, followed by three rinses in DPBS for 5 min each. The slides were then added to permeabilizing solution (1.8 % L-Lysine, 4 % horse serum, and 0.2 % Triton X-100 in DPBS) for 30 min. Slices were circumscribed and incubated overnight with a primary antibody and 4 % horse serum. The next day, slides were rinsed and incubated for 3 h with a fluorescent secondary antibody. A second set of primary and secondary antibodies were used in the case of co-localization staining. Slides were then fixed with Permount mounting media. Primary antibodies include: PKCα, PKCδ, and PKCε mouse 1:500 (Santa Cruz Biotechnology), Claudin-5 mouse 1:200 (Life Technologies),

Author Manuscript Author Manuscript Author Manuscript Author Manuscript

occludin rabbit 1:200 (Life Technologies), VE-Cadherin rabbit 1:150 (Cell Signaling), ZO-1 Alexa Fluor® 488 mouse 1:200 (Life Technologies), Glial Fibrillary Acidic Protein (GFAP) mouse 1:150 (Cell Signaling), GFAP rabbit 1:500 (DAKO, Glostrup, Denmark), Neuronal/glia proteoglycan 2 (NG-2) rabbit 1:500 (Santa Cruz Biotechnology) and Von Willebrand Factor (VWF) rabbit 1:200 (Sigma Aldrich, St. Louis, MO, USA). Secondary antibodies include Alexa Fluor 594 goat anti-mouse 1:1,000 (Life Technologies), Alexa Fluor 594 goat anti-rabbit 1:500 (Life Technologies), Alexa Fluor 488 donkey anti-mouse 1:500 (Life Technologies), and Alexa 488 donkey anti-rabbit 1:1,000 (Life Technologies). Twenty cells per slide were randomly selected, outlined, and measured with ImageJ software (NIH) by an observer blinded to experimental group. Density was adjusted per mean area to give corrected total cell fluorescence normalized to background for claudin-5, occludin, VE-Cadherin, ZO-1, and PKCα, PKCδ, and PKCε. Co-localization was quantified with the ImageJ plugin *Just Another Co-localization plugin* to give Pearson's coefficient for controls and overlap coefficient for treatment groups [40]. For percentage of co-localization, an observer blinded to experimental group counted 100 cells and the ratio of positive cells to total cells was recorded. χ^2 analyses was used to compare between groups.

Statistical Analysis

Biochemical assay data were analyzed using GraphPad Prism 6.0 (GraphPad Software, Inc., La Jolla, CA, USA) by an observer blinded to experimental group. A one-way ANOVA with Tukey's *post-hoc* was used to compare across groups for EB absorbance, western blot analysis, and IHC quantification. Overlap coefficient was calculated via the ImageJ plugin with the following equation: $k^2=k^1\times k2$ with all values adjusted to threshold. Pearson's coefficient was obtained for controls. χ^2 analyses was used to compare the percentages of positive co-localized cells between groups. $p<0.05$ was considered statistically significant for all data analyzed.

Results

Bryostatin-1 Significantly Modulates PKCα and PKCε but not PKCδ Expression After Blast

Bryostatin-1 has previously been shown to be neuroprotective following mild TBI in a murine model by reducing β-secretase and β amyloid production [24]. Furthermore, our lab has published that bryostatin-1 decreases PKCα and increases PKCε following neural injury in an aged-female Sprague–Dawley model [28]. The role bryostatin-1 plays in regulating PKC activity at the neurovascular unit has yet to be determined. We examined perivascular regions of the left prefrontal cortex using quantitative IHC. A significant difference in PKCα was observed between groups ($F(2,24)=7.743$, $p<0.01$) 24 h after injury. *Post-hoc* comparison revealed a significant difference between control and single blast groups ($t=5.043$, $p<0.01$) and between single blast and single blast + bryostatin-1 groups ($t=4.559$, $p<0.01$) (Fig. 2a–g). A significant difference in PKCδ was observed between groups ($F(2,27)=16.73$, $p<0.001$) 24 h after injury. *Post-hoc* comparison revealed a significant difference between control and single blast groups ($t=8.049$, $p<0.001$) and between control and single blast + bryostatin-1 groups ($t=5.292$, $p<0.01$) (Fig. 2h–n). No significant difference was seen between single blast and single blast + bryostatin-1, consistent with the notion that bryostatin-1 negligibly alters PKCδ expression. A significant difference in PKCε

Author Manuscript Author Manuscript Author Manuscript Author Manuscript

was observed between groups (F(2,27)=14.73, $p<0.001$) 24 h after injury. *Post-hoc* comparison revealed a significant difference between control and single blast + bryostatin-1 groups ($t=7.509$, $p<0.001$) and between single blast and single blast + bryostatin-1 groups ($t=5.133$, $p<0.01$) (Fig. 2o–u). We also examined changes in PKC expression using western blot analysis. A significant difference between groups was observed for PKCα (F(2,14)=7.672, $p<0.01$). *Post-hoc* comparison revealed a significant difference between control and single blast ($t=4.576$, $p<0.05$), and between single blast and single blast + bryostatin-1 ($t=5.113$, $p<0.01$) (Fig. 3a). A significant difference between groups was observed for PKCδ (F(2,6)=13.25, $p<0.01$). *Post-hoc* comparison revealed a significant difference between control and single blast ($t=7.197$, p<0.01), and between control and single blast + bryostatin-1 ($t=4.549$, $p<0.05$) (Fig. 3b). A significant difference between groups was observed for PKCε (F(2,15)=10.05, $p<0.01$). *Post-hoc* comparison revealed a significant difference between control and single blast ($t=4.546$, $p<0.05$), and between control and single blast + bryostatin-1 ($t=6.102$, $p<0.01$) (Fig. 3 c).

Bryostatin-1 Maintained BBB Integrity Following Blast Exposure

BBB integrity can be measured by EB extravasation into the brain parenchyma [7]. EB binds to albumin, and albumin does not readily penetrate an intact BBB. NG-2 is a pericyte proteoglycan that is increased during BBB disruption and subsequent neovascularization [41]. Disruption of the BBB has multiple effects including neuroinflammation and formation of reactive oxygen species [42]. A significant difference between groups was observed for EB extravasation 6 h after blast exposure (F(2,7)=7.38, $p<0.05$) for the left prefrontal cortex (Fig. 4a). *Post-hoc* comparison was significant between control and single blast ($t=4.808$, $p<0.05$) and between single blast and single blast + bryostatin-1 ($t=4.347$, $p<0.05$). No significant difference was seen between control and single blast + bryostatin-1. Bryostatin-1 successfully preserved the integrity of the BBB apparent on gross exam of the left hemisphere (Fig. 4b). A significant difference in NG-2 was observed 24 h after blast exposure (F(2,27)=20.42, $p<0.001$) for the left prefrontal cortex (Fig. 4c–h). *Post-hoc* comparison was significant between control and single blast ($t=5.504$, $p<0.01$), and between single blast and single blast + bryostatin-1 ($t=8.961$, $p<0.001$), but not between control and single blast + bryostatin-1.

PKC Modulation Alters Tight Junction Proteins at the Blood Brain Barrier

Activation of PKC isozymes is thought to play a crucial role in BBB disruption [43]. PKCα, in particular, has been linked to redistribution of tight junction proteins leading to increased vascular permeability [44]. PKCα is also known to activate sonic hedgehog protein leading to dysfunctional synthesis of tight junction proteins [45, 46]. Alternatively, increasing PKCε facilitates tight junction protein translocation from the nucleus to the plasma membrane [47]. Gross examination of the neurovascular unit (VWF co-localized with GFAP) revealed histological disruption of the BBB following blast injury but maintenance of barrier integrity when bryostatin-1 was administered following blast exposure (Fig. 5a–c). A significant difference between groups was not observed for Claudin-5 (Fig. 5d–j) using fluorescent IHC. A significant difference between groups was observed for VE-Cadherin (F(2,6)=18.58, $p<0.01$) using western blot. *Post-hoc* comparison revealed a significant difference between control and single blast ($t=4.571$, $p<0.05$), and between control and single blast +

Author Manuscript Author Manuscript Author Manuscript Author Manuscript

bryostatin-1 (t=8.616, p<0.01) (Fig. 6a). A significant difference between groups was observed for occludin (F(2,6)=49.02, p<0.001) using western blot. *Post-hoc* comparison revealed a significant difference between control and single blast (t=6.955, p<0.01), between control and single blast + bryostatin-1 (t=14, p<0.001), and between single blast and single blast + bryostatin-1 (t=7.048, p<0.01) (Fig. 6b). A significant difference between groups was observed for ZO-1 (F(2,26)=35.68, p<0.001) using fluorescent IHC. *Post-hoc* comparison revealed a significant difference between control and single blast + bryostatin-1 (t=11.45, p<0.001), and between single blast and single blast + bryostatin-1 (t=8.553, p<0.001) (Fig. 6c–i). Additionally, a significant difference between groups was observed for VE-Cadherin (F(2,27)=5.9, p<0.05) using fluorescent IHC. *Post-hoc* comparison revealed a significant difference between control and single blast (t=4.016, p<0.05), and between control and single blast + bryostatin-1 (t=4.375, p<0.05) (Fig. 7a–g). A significant difference was also observed between groups for occludin (F(2,27)=79.88, p<0.001). *Post-hoc* comparison revealed a significant difference between control and single blast (t=8.304, p<0.001), between control and single blast + bryostatin-1 (t=17.86, p<0.0001), and between single blast and single blast + bryostatin-1 (t=9.557, p<0.001) (Fig. 7h–n).

PKCα, PKCδ, and PKCε are Co-localized with Endothelial Cells but not Astrocytes after Blast Exposure

The neurovascular unit and the associated BBB consists of endothelial cells, astrocytes, and pericytes that form a structural basement membrane [48]. The unit acts as a consortium that dictates vascular constriction and dilation in response to stimuli [49]. The role of PKC isozymes in mediating changes to vasculature tone following TBI has yet to be elucidated. We examined the extent of co-localization for PKCα, PKCδ, and PKCε with endothelial cells (VWF) or astrocytes (GFAP) in the left prefrontal cortex of control animals and single blast exposed animals 24 h after injury. The Pearson's coefficient for control animals for PKCα and VWF was r=0.395 (Fig. 8a–f). The overlap coefficient for PKCα and VWF after single blast exposure (threshold A=20, threshold B=14) was r=0.954 with $k1$=0.734 and $k2$=1.238 (Fig. 8g–l). The Pearson's coefficient for control animals for PKCα and GFAP was r=0.351 (Fig. 8m–r). The overlap coefficient for PKCα and GFAP after single blast exposure (threshold A=29, threshold B=22) was r=0.379 with $k1$=0.768 and $k2$=0.187 (Fig. 8s–x). The Pearson's coefficient for control animals for PKCα and VWF was r=0.61 (Fig. 9a–f). The overlap coefficient for PKCδ and VWF after single blast exposure (threshold A=34, threshold B=14) was r=0.88 with $k1$ =0.444 and $k2$=1.744 (Fig. 9g–l). The Pearson's coefficient for control animals for PKCδ and GFAP was r=0.029 (Fig. 9m–r). The overlap coefficient for PKCδ and GFAP after single blast exposure (threshold A=52, threshold B=20) was r=0.449 with $k1$=0.227 and $k2$=0.89 (Fig. 9s–x). The Pearson's coefficient for control animals for PKCε and VWF was r=0.004 (Fig. 10a–f). The overlap coefficient for PKCε and VWF after single blast exposure (threshold A=44, threshold B=23) was r=0.978 with $k1$=0.765 and $k2$=1.249 (Fig. 10g–l). The Pearson's coefficient for control animals for PKCε and GFAP was r=0.133 (Fig. 10m–r). The overlap coefficient for PKCε and GFAP after single blast exposure (threshold A=24, threshold B=22) was r=0.394 with $k1$=0.286 and $k2$=0.543 (Fig. 10s–x). We examined the percentage of positive cells for PKCα co-localized with VWF in perivascular regions of the left prefrontal cortex 24 h after injury (Supplementary Fig. 1). The ratio of positively stained cells to total cells for control was 18/

Author Manuscript Author Manuscript Author Manuscript Author Manuscript

100, for blast-exposed animals 57/100, and for blast exposed animals treated with bryostatin-1 36/100. χ^2=20.595 with two degrees of freedom and a two-tailed *p* value equal to 0.0001.

Discussion

Bryostatin-1 has been successfully used in numerous animal models of neural injury including TBI, ischemic stroke, auditory neurodegeneration, and Alzheimer's disease and is currently under investigation in clinical trials [50, 51, 24, 52]. Recent findings have shown that secondary injury mechanisms such as neuroinflammation, endoplasmic reticulum stress, and PKC activity are conserved despite the type of injury [53–55]. The timing of activity might vary but the pathways are similar and theoretically targeted in a similar fashion. For example, bryostatin-1 protects against loss of pre-synaptic synaptophysin and loss of post-synaptic spinophylin following TBI in mice [24]. In an aged-female Sprague– Dawley stroke model, bryostatin-1 improved survival and reduced ischemic damage [28]. Likewise, bryostatin-1 decreased apoptosis and prevented deficits in synaptogenesis in a global model of cerebral ischemia [50, 56]. Despite the different injury models bryostatin-1 was a successful therapeutic because it upregulates PKC activity early and downregulates activity when used at excess doses or at chronic time points [57]. At the dose used in this study, it is possible that an early activation of PKCα is followed by a drastic downregulation observed at 24 h. PKCε may also be increased not only due to upregulation but also from increased synthesis [27]. Future studies will be required to look at PKC changes at both earlier time points and also the beneficial effects of bryostatin-1 when administered at subacute time points. In Alzheimer's disease, early upregulation of PKC activity enhances neuronal repair and decreases amyloid-mediated degeneration while maintaining long-term potentiation [58, 59]. In addition, bryostatin-1 facilitates neurite outgrowth, maintains cognitive function [52], and enhances synaptic connectivity and spatial learning [34]. For affective disorders, bryostatin-1 downregulates ERK-dependent PKC activity at late time points, which can have beneficial effects for treating substance abuse, depression, and aversive emotional memories [51, 60]. Similar molecular PKC targets appear to be altered in TBI [14].The potential for bryostatin-1 as a treatment for TBI warrants further investigation. The necessity for different dosing strategies as well as altering the timing of dosing must be carefully considered in a series of future studies. Furthermore, specific activation of select isozymes will offer compelling insight into their protective properties following TBI. In this study, we examined how a single 2.5 mg/kg dose of bryostatin-1 affects BBB integrity acutely following blast-induced TBI.

We found that a single moderate TBI significantly increased EB extravasation into the left prefrontal cortex 6 h after injury. Bryostatin-1 administration ameliorated this disruption. A potential mechanism by which this occurs is through regulation of PKCα and PKCε, which subsequently increases the tight junction proteins VE-Cadherin, occludin, and ZO-1 at the BBB. It has been previously shown in an ischemic stroke model that inhibiting PKCα increases the tight junction proteins ZO-1, occludin, and VE-Cadherin [61]. PKCα has limited regulatory function for claudin-5 accounting for the non-significant findings observed. Tight junction proteins overall are essential for maintaining limited and selective permeability into the brain parenchyma and preventing neuroinflammation [62]. A switch to

Author Manuscript Author Manuscript Author Manuscript Author Manuscript

PKCα activation following TBI has been shown to accelerate neuroinflammation [63]. Our data show that bryostatin-1 decreased levels of PKCα when given after blast. A separate isozyme, PKCδ, mediates vasoconstriction, but its role in tight junction disruption is poorly understood [64]. Our data show that bryostatin-1 had a negligible effect on PKCδ levels. Another isozyme, PKCε, is associated with neuroprotection in various models of brain injury [65]. Bryostatin-1 was previously shown to regulate tight junction proteins in vitro via modulation of PKCe [66]. PKCe is essential for exportation of zona occluden proteins to the site of functional activity [47]. We found that bryostatin-1 significantly elevated PKCε when administered after blast injury.

Increasing VE-Cadherin, occludin, and ZO-1 strengthens the BBB therefore maintaining its integrity [67]. Other therapeutic approaches for TBI such as hyperbaric oxygen and sevoflurane were previously shown to significantly increase tight junction protein expression [68, 69]. Our data provide compelling evidence that bryostatin-1 also increases tight junction proteins leading to maintenance of the BBB and decreased permeability after blast injury. Future work will examine the functional capacity of these tight junction proteins as well as their efficient means of trafficking [70]. Utilizing in vitro modeling with astrocyte and endothelial co-culture may represent an effective way to examine functional capacity [71]. Designing an effective in vitro model of blast TBI and BBB dynamics is an area requiring focused investigation [72, 73]. Another avenue requiring further investigation is how changes in PKC function affect the gliovascular unit. Our data show that PKC changes were localized to the endothelial cells not glia. What has yet to be discovered is how cytokines released from endothelial cells may alter the surrounding gliovascular unit [74]. In order to investigate this important area, specific PKC modulators such as (Alphatomega; H-FKKQGSFAKKK-NH(2)) for PKCα and the PKCε peptide activator must be used in future investigative studies [75, 76]. A malfunctioning gliovascular unit can contribute to chronic neurodegeneration [77].

An area of ongoing research is how the progression of acute BBB disruption leads to chronic detrimental outcomes. Subtle changes can occur in a young developing brain post TBI that often take years to manifest into symptoms [78]. Microbleeds from a disrupted BBB following TBI can cause long-term negative outcomes such as glial scarring and white matter degeneration [79–81]. These markers of injury have been associated with mid-to-late life diseases such as chronic traumatic encephalopathy, autoimmune encephalomyelitis, vascular dementia, and early-onset Alzheimer's disease [82–84]. Interestingly, stabilization of the BBB through PKC modulation decreases chronic negative effects acutely [85]. If BBB disruption does occur, calcium imbalance triggers a host of downstream events. Current understanding indicates that glia communicate with neurons through calcium signaling, and calcium signaling is often disrupted following TBI [86]. Disrupted calcium signaling can lead to activation of endoplasmic reticulum stress and mitochondrial dysfunction [87]. Long-term outcomes include the formation of reactive oxygen species, amyloid pathology, and tau hyperphosphorylation [88]. PKC isozymes are known tau kinases that are increased in neurodegenerative disease [89]. Long-term bryostatin-1 treatment has been shown to modulate tau hyperphosphorylation in a murine model of dementia [90, 51]. A large prospective cohort study has recently shown that veterans diagnosed with TBI have a 1.57 adjusted hazard ratio for the onset of dementia compared to controls [91]. Ongoing work

Author Manuscript Author Manuscript Author Manuscript Author Manuscript

will investigate the long-term role bryostatin-1 treatment plays in preventing neurodegeneration following repetitive blast exposure. Appropriate dosing strategies will be carefully developed for single and repetitive injury. The effects of bryostatin-1 are likely twofold: protection of BBB acutely and preservation of neuronal stability chronically. Timing and appropriate dosing is a necessity to tease out the most appropriate protective treatment windows. PKC modulation offers a promising therapeutic approach for preventing the chronic sequelae associated with neurotrauma.

Supplementary Material

Refer to Web version on PubMed Central for supplementary material.

Acknowledgments

The authors would like to thank Ryan W. Holt for his help with IHC and western blot analysis. We thank Diana Richardson CDC/NIOSH for tissue preparation for IHC. The authors also thank Dr. Rae Matsumoto and Dr. Steven Frisch for use of western blot resources in their respective laboratories. We thank James E. Robson and Peter Bennett for construction of the blast model and Dr. Robert Gettens and Nic St. John for design of the blast model. A Research Funding and Development Grant (RFDG) from the West Virginia University Health Sciences Center Office of Research and Graduate Education supported this work along with WVU Department of Neurosurgery. R.C.T. was supported by a NIH training grant (GM08174).

Abbreviations

CTRL	Control
GFAP	Glial fibrillary acidic protein
IHC	Immunohistochemistry
PKC	Protein kinase C
SB	Single blast
SB + Bryo	Single blast + bryostatin-1
VWF	Von Willebrand factor

References

1. Kou Z, Vandevord PJ. Traumatic white matter injury and glial activation: from basic science to clinics. Glia. 2014
2. Schneider EB, Sur S, Raymont V, Duckworth J, Kowalski RG, Efron DT, Hui X, Selvarajah S, Hambridge HL, Stevens RD. Functional recovery after moderate/severe traumatic brain injury: a role for cognitive reserve? Neurology. 2014; 82(18):1636–1642. [PubMed: 24759845]
3. Puvenna V, Brennan C, Shaw G, Yang C, Marchi N, Bazarian JJ, Merchant-Borna K, Janigro D. Significance of ubiquitin carboxy-terminal hydrolase l1 elevations in athletes after subconcussive head hits. PLoS One. 2014; 9(5):e96296. [PubMed: 24806476]
4. Simard JMMDPD, Pampori A, Keledjian K, Tosun C, Schwartzbauer G, Ivanova S, Gerzanich V. Exposure of the thorax to a sublethal blast wave causes a hydrodynamic pulse that leads to perivenular inflammation in the brain. J Neurotrauma. 2014
5. Hue CD, Cao S, Dale Bass CR, Meaney DF, Morrison B 3rd. Repeated primary blast injury causes delayed recovery, but not additive disruption, in an in vitro blood–brain barrier model. J Neurotrauma. 2014; 31(10):951–960. [PubMed: 24372353]

Author Manuscript Author Manuscript Author Manuscript Author Manuscript

6. Yeoh S, Bell ED, Monson KL. Distribution of blood–brain barrier disruption in primary blast injury. Ann Biomed Eng. 2013; 41(10):2206–2214. [PubMed: 23568152]
7. Abdul-Muneer PM, Schuetz H, Wang F, Skotak M, Jones J, Gorantla S, Zimmerman MC, Chandra N, Haorah J. Induction of oxidative and nitrosative damage leads to cerebrovascular inflammation in an animal model of mild traumatic brain injury induced by primary blast. Free Radic Biol Med. 2013; 60:282–291. [PubMed: 23466554]
8. Perez-Polo JR, Rea HC, Johnson KM, Parsley MA, Unabia GC, Xu G, Infante SK, Dewitt DS, Hulsebosch CE. Inflammatory consequences in a rodent model of mild traumatic brain injury. J Neurotrauma. 2013; 30(9):727–740. [PubMed: 23360201]
9. Readnower RD, Chavko M, Adeeb S, Conroy MD, Pauly JR, McCarron RM, Sullivan PG. Increase in blood–brain barrier permeability, oxidative stress, and activated microglia in a rat model of blast-induced traumatic brain injury. J Neurosci Res. 2010; 88(16):3530–3539. [PubMed: 20882564]
10. Yang K, Taft WC, Dixon CE, Todaro CA, Yu RK, Hayes RL. Alterations of protein kinase C in rat hippocampus following traumatic brain injury. J Neurotrauma. 1993; 10(3):287–295. [PubMed: 8258841]
11. Padmaperuma B, Mark R, Dhillon HS, Mattson MP, Prasad MR. Alterations in brain protein kinase C after experimental brain injury. Brain Res. 1996; 714(1–2):19–26. [PubMed: 8861605]
12. Muscella A, Marsigliante S, Verri T, Urso L, Dimitri C, Botta G, Paulmichl M, Beck-Peccoz P, Fugazzola L, Storelli C. PKC-epsilon-dependent cytosol-to-membrane translocation of pendrin in rat thyroid PC Cl3 cells. J Cell Physiol. 2008; 217(1):103–112. [PubMed: 18459119]
13. Chen T, Cao L, Dong W, Luo P, Liu W, Qu Y, Fei Z. Protective effects of mGluR5 positive modulators against traumatic neuronal injury through PKC-dependent activation of MEK/ERK pathway. Neurochem Res. 2012; 37(5):983–990. [PubMed: 22228200]
14. Luo P, Chen T, Zhao Y, Zhang L, Yang Y, Liu W, Li S, Rao W, Dai S, Yang J, Fei Z. Postsynaptic scaffold protein Homer 1a protects against traumatic brain injury via regulating group I metabotropic glutamate receptors. Cell Death Dis. 2014; 5:e1174. [PubMed: 24722299]
15. Geddes-Klein DM, Serbest G, Mesfin MN, Cohen AS, Meaney DF. Pharmacologically induced calcium oscillations protect neurons from increases in cytosolic calcium after trauma. J Neurochem. 2006; 97(2):462–474. [PubMed: 16539664]
16. Roh DH, Yoon SY, Seo HS, Kang SY, Moon JY, Song S, Beitz AJ, Lee JH. Sigma-1 receptor-induced increase in murine spinal NR1 phosphorylation is mediated by the PKCαlpha and epsilon, but not the PKCzeta, isoforms. Neurosci Lett. 2010; 477(2):95–99. [PubMed: 20417251]
17. Giordano G, Sanchez-Perez AM, Burgal M, Montoliu C, Costa LG, Felipo V. Chronic exposure to ammonia induces isoform-selective alterations in the intracellular distribution and NMDA receptor-mediated translocation of protein kinase C in cerebellar neurons in culture. J Neurochem. 2005; 92(1):143–157. [PubMed: 15606904]
18. Pandya JD, Nukala VN, Sullivan PG. Concentration dependent effect of calcium on brain mitochondrial bioenergetics and oxidative stress parameters. Front Neuroenerg. 2013; 5:10.
19. Yang K, Taft WC, Dixon CE, Yu RK, Hayes RL. Endogenous phosphorylation of a 61,000 dalton hippocampal protein increases following traumatic brain injury. J Neurotrauma. 1994; 11(5):523–532. [PubMed: 7861445]
20. Karasu A, Aras Y, Sabanci PA, Saglam G, Izgi N, Biltekin B, Barak T, Hepgul KT, Kaya M, Bilir A. The effects of protein kinase C activator phorbol dibutyrate on traumatic brain edema and aquaporin-4 expression.Ulusal travma ve acil cerrahi dergisi. Turk J Trauma Emerg Surg TJTES. 2010; 16(5):390–394.
21. Kim YA, Park SL, Kim MY, Lee SH, Baik EJ, Moon CH, Jung YS. Role of PKCbetaII and PKCdelta in blood–brain barrier permeability during aglycemic hypoxia. Neurosci Lett. 2010; 468(3):254–258. [PubMed: 19900507]
22. Kizub IV, Klymenko KI, Soloviev AI. Protein kinase C in enhanced vascular tone in diabetes mellitus. Int J Cardiol. 2014; 174(2):230–242. [PubMed: 24794552]
23. Lin HW, Della-Morte D, Thompson JW, Gresia VL, Narayanan SV, Defazio RA, Raval AP, Saul I, Dave KR, Morris KC, Si ML, Perez-Pinzon MA. Differential effects of delta and epsilon protein kinase C in modulation of postischemic cerebral blood flow. Adv Exp Med Biol. 2012; 737:63–69. [PubMed: 22259083]

Author Manuscript Author Manuscript Author Manuscript Author Manuscript

24. Zohar O, Lavy R, Zi X, Nelson TJ, Hongpaisan J, Pick CG, Alkon DL. PKC activator therapeutic for mild traumatic brain injury in mice. Neurobiol Dis. 2011; 41(2):329–337. [PubMed: 20951803]
25. Lim CS, Alkon DL. PKCepsilon promotes HuD-mediated neprilysin mRNA stability and enhances neprilysin-induced Abeta degradation in brain neurons. PLoS One. 2014; 9(5):e97756. [PubMed: 24848988]
26. Xu C, Liu QY, Alkon DL. PKC activators enhance GABAergic neurotransmission and paired-pulse facilitation in hippocampal CA1 pyramidal neurons. Neuroscience. 2014; 268:75–86. [PubMed: 24637095]
27. Hongpaisan J, Sun MK, Alkon DL. PKC epsilon activation prevents synaptic loss, Abeta elevation, and cognitive deficits in Alzheimer's disease transgenic mice. J Neurosci Off J Soc Neurosci. 2011; 31(2):630–643.
28. Tan Z, Turner RC, Leon RL, Li X, Hongpaisan J, Zheng W, Logsdon AF, Naser ZJ, Alkon DL, Rosen CL, Huber JD. Bryostatin improves survival and reduces ischemic brain injury in aged rats after acute ischemic stroke. Stroke J Cereb Circ. 2013; 44(12):3490–3497.
29. Turner RC, Naser ZJ, Logsdon AF, DiPasquale KH, Jackson GJ, Robson MJ, Gettens RT, Matsumoto RR, Huber JD, Rosen CL. Modeling clinically relevant blast parameters based on scaling principles produces functional histological deficits in rats. Exp Neurol. 2013; 248:520–529. [PubMed: 23876514]
30. Morrow CM, Mruk D, Cheng CY, Hess RA. Claudin and occludin expression and function in the seminiferous epithelium. Philos Trans R Soc Lond B Biol Sci. 2010; 365(1546):1679–1696. [PubMed: 20403878]
31. Goncalves A, Leal E, Paiva A, Teixeira Lemos E, Teixeira F, Ribeiro CF, Reis F, Ambrosio AF, Fernandes R. Protective effects of the dipeptidyl peptidase IV inhibitor sitagliptin in the blood-retinal barrier in a type 2 diabetes animal model. Diabetes Obes Metab. 2012; 14(5):454–463. [PubMed: 22151893]
32. Sun MK, Alkon DL. Bryostatin-1: pharmacology and therapeutic potential as a CNS drug. CNS Drug Rev. 2006; 12(1):1–8. [PubMed: 16834754]
33. Berkow RL, Schlabach L, Dodson R, Benjamin WH Jr, Pettit GR, Rustagi P, Kraft AS. In vivo administration of the anticancer agent bryostatin 1 activates platelets and neutrophils and modulates protein kinase C activity. Cancer Res. 1993; 53(12):2810–2815. [PubMed: 8504423]
34. Sun MK, Hongpaisan J, Lim CS, Alkon DL. Bryostatin-1 restores hippocampal synapses and spatial learning and memory in adult fragile x mice. J Pharmacol Exp Ther. 2014; 349(3):393–401. [PubMed: 24659806]
35. Turner RC, Naser ZJ, Bailes JE, Smith DW, Fisher JA, Rosen CL. Effect of slosh mitigation on histologic markers of traumatic brain injury: laboratory investigation. J Neurosurg. 2012; 117(6): 1110–1118. [PubMed: 22998060]
36. Bass CR, Panzer MB, Rafaels KA, Wood G, Shridharani J, Capehart B. Brain injuries from blast. Ann Biomed Eng. 2012; 40(1):185–202. [PubMed: 22012085]
37. Panzer MB, Wood GW, Bass CR. Scaling in neurotrauma: how do we apply animal experiments to people? Exp Neurol. 2014
38. Yen LF, Wei VC, Kuo EY, Lai TW. Distinct patterns of cerebral extravasation by Evans blue and sodium fluorescein in rats. PLoS One. 2013; 8(7):e68595. [PubMed: 23861924]
39. Dinapoli VA, Benkovic SA, Li X, Kelly KA, Miller DB, Rosen CL, Huber JD, O'Callaghan JP. Age exaggerates proinflammatory cytokine signaling and truncates signal transducers and activators of transcription 3 signaling following ischemic stroke in the rat. Neuroscience. 2010; 170(2):633–644. [PubMed: 20633608]
40. Bolte S, Cordelieres FP. A guided tour into subcellular colocalization analysis in light microscopy. J Microsc. 2006; 224(Pt 3):213–232. [PubMed: 17210054]
41. Girolamo F, Dallatomasina A, Rizzi M, Errede M, Walchli T, Mucignat MT, Frei K, Roncali L, Perris R, Virgintino D. Diversified expression of NG2/CSPG4 isoforms in glioblastoma and human foetal brain identifies pericyte subsets. PLoS One. 2013; 8(12): e84883. [PubMed: 24386429]

Author Manuscript Author Manuscript Author Manuscript Author Manuscript

42. Abdul-Muneer PM, Chandra N, Haorah J. Interactions of oxidative stress and neurovascular inflammation in the pathogenesis of traumatic brain injury. Mol Neurobiol. 2014
43. Shao B, Bayraktutan U. Hyperglycaemia promotes human brain microvascular endothelial cell apoptosis via induction of protein kinase C-ssI and prooxidant enzyme NADPH oxidase. Redox Biol. 2014; 2:694–701. [PubMed: 24936444]
44. Stamatovic SM, Dimitrijevic OB, Keep RF, Andjelkovic AV. Protein kinase Calpha-RhoA cross-talk in CCL2-induced alterations in brain endothelial permeability. J Biol Chem. 2006; 281(13): 8379–8388. [PubMed: 16439355]
45. Xia YP, He QW, Li YN, Chen SC, Huang M, Wang Y, Gao Y, Huang Y, Wang MD, Mao L, Hu B. Recombinant human sonic hedgehog protein regulates the expression of ZO-1 and occludin by activating angiopoietin-1 in stroke damage. PLoS One. 2013; 8(7):e68891. [PubMed: 23894369]
46. Guo D, Standley C, Bellve K, Fogarty K, Bao ZZ. Protein kinase Calpha and integrin-linked kinase mediate the negative axon guidance effects of Sonic hedgehog. Mol Cell Neurosci. 2012; 50(1): 82–92. [PubMed: 22521536]
47. Chamorro D, Alarcon L, Ponce A, Tapia R, Gonzalez-Aguilar H, Robles-Flores M, Mejia-Castillo T, Segovia J, Bandala Y, Juaristi E, Gonzalez-Mariscal L. Phosphorylation of zona occludens-2 by protein kinase C epsilon regulates its nuclear exportation. Mol Biol Cell. 2009; 20(18):4120–4129. [PubMed: 19625451]
48. Amtul Z, Hepburn JD. Protein markers of cerebrovascular disruption of neurovascular unit: immunohistochemical and imaging approaches. Rev Neurosci. 2014
49. Muoio V, Persson PB, Sendeski MM. The neurovascular unit -concept review. Acta Physiol. 2014; 210(4):790–798.
50. Sun MK, Hongpaisan J, Alkon DL. Postischemic PKC activation rescues retrograde and anterograde long-term memory. Proc Natl Acad Sci U S A. 2009; 106(34):14676–14680. [PubMed: 19667190]
51. Sun MK, Alkon DL. The “Memory Kinases”: roles of PKC isoforms in signal processing and memory formation. Prog Mol Biol Transl Sci. 2014; 122:31–59. [PubMed: 24484697]
52. Lallemend F, Hadjab S, Hans G, Moonen G, Lefebvre PP, Malgrange B. Activation of protein kinase CbetaI constitutes a new neurotrophic pathway for deafferented spiral ganglion neurons. J Cell Sci. 2005; 118(Pt 19):4511–4525. [PubMed: 16179609]
53. Wu J, Zhao Z, Sabirzhanov B, Stoica BA, Kumar A, Luo T, Skovira J, Faden AI. Spinal cord injury causes brain inflammation associated with cognitive and affective changes: role of cell cycle pathways. J Neurosci Off J Soc Neurosci. 2014; 34(33):10989–11006.
54. Lucke-Wold BP, Turner RC, Logsdon AF, Simpkins JW, Alkon DL, Smith KE, Chen YW, Tan Z, Huber JD, Rosen CL. Common mechanisms of Alzheimer’s disease and ischemic stroke: the role of protein kinase C in the progression of age-related neurodegeneration. J Alzheimers Dis JAD. 2014
55. Hoozemans JJ, Scheper W. Endoplasmic reticulum: the unfolded protein response is tangled in neurodegeneration. Int J Biochem Cell Biol. 2012; 44(8):1295–1298. [PubMed: 22564438]
56. Sun MK, Hongpaisan J, Nelson TJ, Alkon DL. Poststroke neuronal rescue and synaptogenesis mediated in vivo by protein kinase C in adult brains. Proc Natl Acad Sci U S A. 2008; 105(36): 13620–13625. [PubMed: 18768786]
57. Sun MK, Alkon DL. Cerebral ischemia-induced difference in sensitivity to depression and potential therapeutics in rats. Behav Pharmacol. 2013; 24(3):222–228. [PubMed: 23591125]
58. Kim H, Han SH, Quan HY, Jung YJ, An J, Kang P, Park JB, Yoon BJ, Seol GH, Min SS. Bryostatin-1 promotes long-term potentiation via activation of PKCαlpha and PKCepsilon in the hippocampus. Neuroscience. 2012; 226:348–355. [PubMed: 22986161]
59. Nelson TJ, Alkon DL. Neuroprotective versus tumorigenic protein kinase C activators. Trends Biochem Sci. 2009; 34(3):136–145. [PubMed: 19233655]
60. Mogha A, Guariglia SR, Debata PR, Wen GY, Banerjee P. Serotonin 1A receptor-mediated signaling through ERK and PKCαlpha is essential for normal synaptogenesis in neonatal mouse hippocampus. Transl Psychiatry. 2012; 2:e66. [PubMed: 22832728]

Author Manuscript Author Manuscript Author Manuscript Author Manuscript

61. Yu H, Wang P, An P, Xue Y. Recombinant human angiopoietin-1 ameliorates the expressions of ZO-1, occludin, VE-cadherin, and PKCαlpha signaling after focal cerebral ischemia/ reperfusion in rats. J Mol Neurosci MN. 2012; 46(1):236–247. [PubMed: 21710361]
62. Chodobski A, Zink BJ, Szmydynger-Chodobska J. Blood- brain barrier pathophysiology in traumatic brain injury. Transl Stroke Res. 2011; 2(4):492–516. [PubMed: 22299022]
63. Dai SS, Zhou YG, Li W, An JH, Li P, Yang N, Chen XY, Xiong RP, Liu P, Zhao Y, Shen HY, Zhu PF, Chen JF. Local glutamate level dictates adenosine A2A receptor regulation of neuroinflammation and traumatic brain injury. J Neurosci Off J Soc Neurosci. 2010; 30(16):5802–5810.
64. Novokhatska T, Tishkin S, Dosenko V, Boldyriev A, Ivanova I, Strielkov I, Soloviev A. Correction of vascular hypercontractility in spontaneously hypertensive rats using shRNAs-induced delta protein kinase C gene silencing. Eur J Pharmacol. 2013; 718(1-3):401–407. [PubMed: 23973649]
65. Feng S, Li D, Li Y, Yang X, Han S, Li J. Insight into hypoxic preconditioning and ischemic injury through determination of nPKCepsilon-interacting proteins in mouse brain. Neurochem Int. 2013; 63(2):69–79. [PubMed: 23665338]
66. Yoo J, Nichols A, Mammen J, Calvo I, Song JC, Worrell RT, Matlin K, Matthews JB. Bryostatin-1 enhances barrier function in T84 epithelia through PKC-dependent regulation of tight junction proteins. Am J Physiol Cell Physiol. 2003; 285(2):C300–C309. [PubMed: 12660149]
67. Liu W, Wang P, Shang C, Chen L, Cai H, Ma J, Yao Y, Shang X, Xue Y. Endophilin-1 regulates blood–brain barrier permeability by controlling ZO-1 and occludin expression via the EGFR-ERK1/2 pathway. Brain Res. 2014
68. Thal SC, Luh C, Schaible EV, Timaru-Kast R, Hedrich J, Luhmann HJ, Engelhard K, Zehendner CM. Volatile anesthetics influence blood–brain barrier integrity by modulation of tight junction protein expression in traumatic brain injury. PLoS One. 2012; 7(12):e50752. [PubMed: 23251381]
69. Chen X, Duan XS, Xu LJ, Zhao JJ, She ZF, Chen WW, Zheng ZJ, Jiang GD. Interleukin-10 mediates the neuroprotection of hyperbaric oxygen therapy against traumatic brain injury in mice. Neuroscience. 2014; 266:235–243. [PubMed: 24291771]
70. McCaffrey G, Davis TP. Physiology and pathophysiology of the blood–brain barrier: P-glycoprotein and occludin trafficking as therapeutic targets to optimize central nervous system drug delivery. J Investig Med Off Publ Am Fed Clin Res. 2012; 60(8):1131–1140.
71. Yang L, Shah KK, Abbruscato TJ. An in vitro model of ischemic stroke. Methods Mol Biol. 2012; 814:451–466. [PubMed: 22144325]
72. Effgen GB, Vogel EW 3rd, Lynch KA, Lobel A, Hue CD, Meaney DF, Bass CR, Morrison B 3rd. Isolated primary blast alters neuronal function with minimal cell death in organotypic hippocampal slice cultures. J Neurotrauma. 2014; 31(13):1202–1210. [PubMed: 24558968]
73. Arun P, Abu-Taleb R, Valiyaveettil M, Wang Y, Long JB, Nambiar MP. Extracellular cyclophilin A protects against blast-induced neuronal injury. Neurosci Res. 2013; 76(1–2):98–100. [PubMed: 23511555]
74. Alves JL. Blood–brain barrier and traumatic brain injury. J Neurosci Res. 2014; 92(2):141–147. [PubMed: 24327344]
75. Kang JH, Asai D, Yamada S, Toita R, Oishi J, Mori T, Niidome T, Katayama Y. A short peptide is a protein kinase C (PKC) alpha-specific substrate. Proteomics. 2008; 8(10):2006–2011. [PubMed: 18425734]
76. Teng JC, Kay H, Chen Q, Adams JS, Grilli C, Guglielmello G, Zambrano C, Krass S, Bell A, Young LH. Mechanisms related to the cardioprotective effects of protein kinase C epsilon (PKC epsilon) peptide activator or inhibitor in rat ischemia/reperfusion injury. Naunyn Schmiedeberg's Arch Pharmacol. 2008; 378(1):1–15. [PubMed: 18496674]
77. Barzilai A. The interrelations between malfunctioning DNA damage response (DDR) and the functionality of the neuro-gliovascular unit. DNA Repair. 2013; 12(8):543–557. [PubMed: 23706773]
78. Adelson PD, Fellows-Mayle W, Kochanek PM, Dixon CE. Morris water maze function and histologic characterization of two age-at-injury experimental models of controlled cortical impact in the immature rat. Childs Nerv Syst CHNS Off J Int Soc Pediatr Neurosurg. 2013; 29(1):43–53.

Author Manuscript Author Manuscript Author Manuscript Author Manuscript

79. Glushakova OY, Johnson D, Hayes RL. Delayed increases in microvascular pathology after experimental traumatic brain injury are associated with prolonged inflammation, blood–brain barrier disruption, and progressive white matter damage. J Neurotrauma. 2014
80. Lucke-Wold BP, Turner RC, Logsdon AF, Bailes JE, Huber JD, Rosen CL. Linking traumatic brain injury to chronic traumatic encephalopathy: identification of potential mechanisms leading to neurofibrillary tangle development. J Neurotrauma. 2014
81. Wu J, Pajoohesh-Ganji A, Stoica BA, Dinizo M, Guanciale K, Faden AI. Delayed expression of cell cycle proteins contributes to astroglial scar formation and chronic inflammation after rat spinal cord contusion. J Neuroinflammation. 2012; 9:169. [PubMed: 22784881]
82. Stein TD, Alvarez VE, McKee AC. Chronic traumatic encephalopathy: a spectrum of neuropathological changes following repetitive brain trauma in athletes and military personnel. Alzheimers Res Ther. 2014; 6(1):4. [PubMed: 24423082]
83. Turner RC, Lucke-Wold BP, Robson MJ, Omalu BI, Petraglia AL, Bailes JE. Repetitive traumatic brain injury and development of chronic traumatic encephalopathy: a potential role for biomarkers in diagnosis, prognosis, and treatment? Front Neurol. 2012; 3:186. [PubMed: 23335911]
84. Marcelo A, Bix G. The potential role of perlecan domain Vas novel therapy in vascular dementia. Metab Brain Dis. 2014
85. Lanz TV, Becker S, Osswald M, Bittner S, Schuhmann MK, Opitz CA, Gaikwad S, Wiestler B, Litzenburger UM, Sahm F, Ott M, Iwantscheff S, Grabitz C, Mittelbronn M, von Deimling A, Winkler F, Meuth SG, Wick W, Platten M. Protein kinase Cbeta as a therapeutic target stabilizing blood–brain barrier disruption in experimental autoimmune encephalomyelitis. Proc Natl Acad Sci U S A. 2013; 110(36):14735–14740. [PubMed: 23959874]
86. De Bock M, Decrock E, Wang N, Bol M, Vinken M, Bultynck G, Leybaert L. The dual face of connexin-based astroglial Ca communication: a key player in brain physiology and a prime target in pathology. Biochim Biophys Acta. 2014
87. Naviaux RK. Metabolic features of the cell danger response. Mitochondrion. 2014; 16:7–17. [PubMed: 23981537]
88. Eckert A, Nisbet R, Grimm A, Gotz J. March separate, strike together - role of phosphorylated TAU in mitochondrial dysfunction in Alzheimer's disease. Biochim Biophys Acta. 2013
89. Kamat PK, Rai S, Swarnkar S, Shukla R, Nath C. Molecular and cellular mechanism of okadaic acid (OKA)-induced neurotoxicity: a novel tool for Alzheimer's disease therapeutic application. Mol Neurobiol. 2014
90. Ekinci FJ, Shea TB. Selective activation by bryostatin-1 demonstrates unique roles for PKC epsilon in neurite extension and tau phosphorylation. Int J Dev Neurosci Off J Int Soc Dev Neurosci. 1997; 15(7):867–874.
91. Barnes DE, Kaup A, Kirby KA, Byers AL, Diaz-Arrastia R, Yaffe K. Traumatic brain injury and risk of dementia in older veterans. Neurology. 2014; 83(4):312–319. [PubMed: 24966406]

Author Manuscript Author Manuscript Author Manuscript Author Manuscript

TEST: / TIME:	Evan's Blue	IHC	Western Blot •(Tight Junction Proteins)	Microvessel Isolation •(PKC Isozymes)
6 hour	✓	–	–	–
24 hour	–	✓	✓	✓

Fig. 1.
Table showing the experimental techniques used for each time point

Author Manuscript Author Manuscript Author Manuscript Author Manuscript

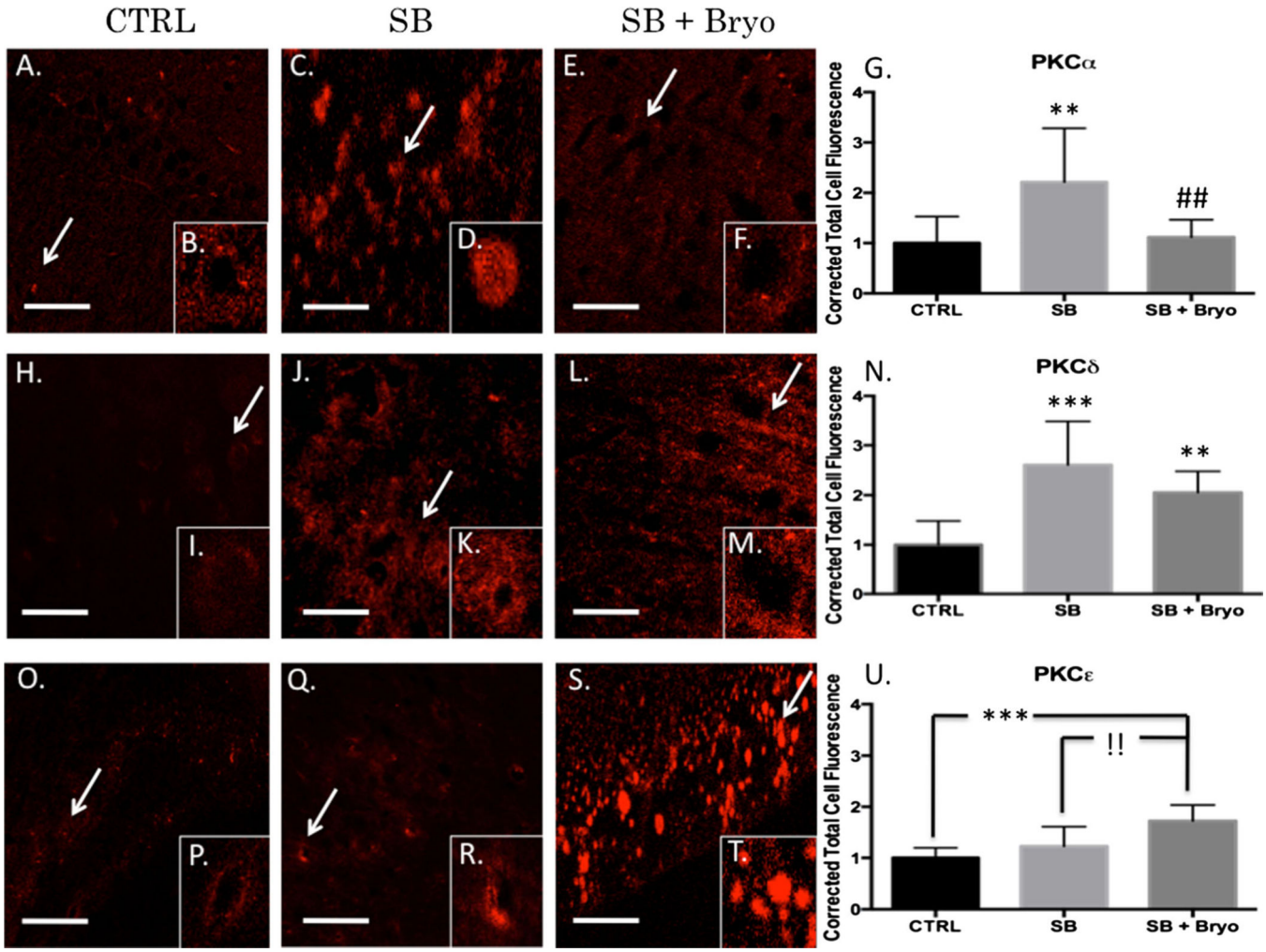

Fig. 2.

Bryostatin-1 decreases PKCα and increases PKCε 24 h after blast exposure. Our data show that bryostatin-1 has a profound effect after blast traumatic brain injury using fluorescent IHC. Scale bar=100 μm in left prefrontal cortex. PKCα control (**a**) with inlay (**b**) compared to single blast exposure (**c**) with inlay (**d**), and single blast exposure + bryostatin-1 (**e**) with inlay (**f**) showed significant difference between groups. *Post-hoc* comparison between control and single blast (**p<0.01) and between single blast and single blast + bryostatin-1 (##p<0.01) as depicted in bar graph (**g**). PKCγ control (**h**) with inlay (**i**) compared to single blast exposure (**j**) with inlay (**k**), and single blast exposure + bryostatin-1 (**l**) with inlay (**m**) showed significant difference between groups. *Post-hoc* comparison between control and single blast (***p<0.001) and between control and single blast + bryostatin-1 (**p<0.01) as depicted in bar graph (**n**). PKCε control (**o**) with inlay (**p**) compared to single blast exposure (**q**) with inlay (**r**), and single blast exposure + bryostatin-1 (**s**) with inlay (**t**) showed a significant difference between groups. *Post-hoc* comparison between control and single blast + bryostatin-1 (***p<0.001) and between single blast and single blast + bryostatin-1 (!! p<0.01) as depicted in bar graph (**u**)

Author Manuscript Author Manuscript Author Manuscript Author Manuscript

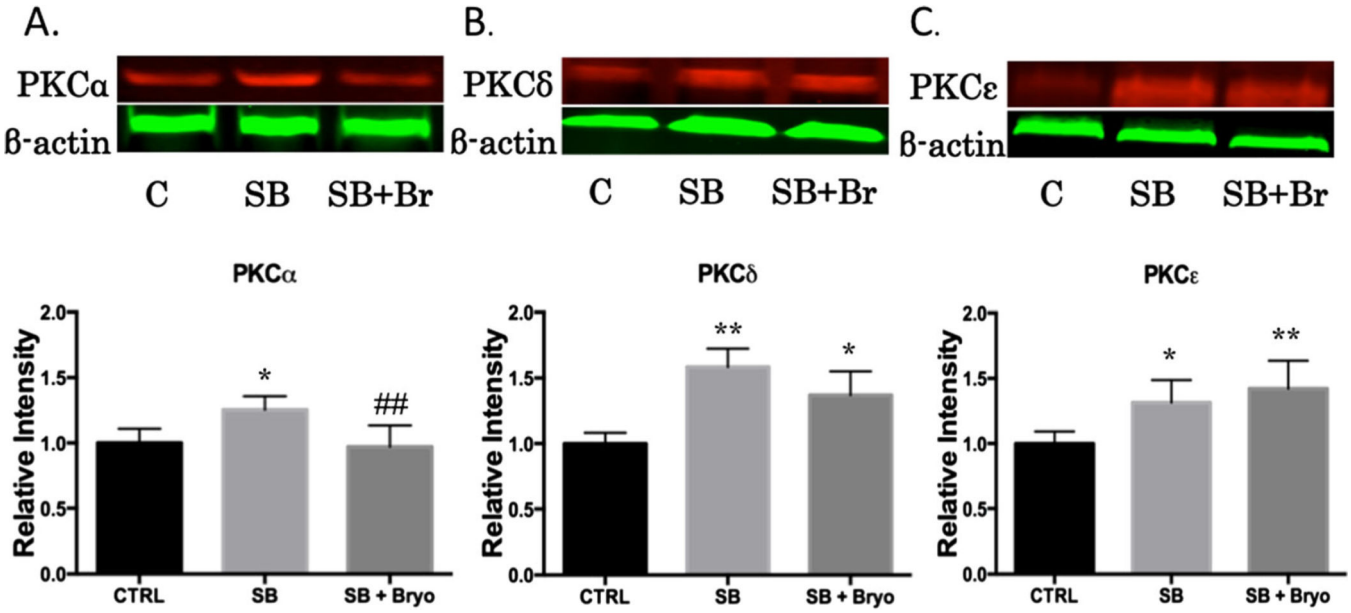

Fig. 3.

Bryostatin-1 is a potent PKC modulator. It has been used to regulate PKC activity in a time-specific manner for multiple neural injury models. Protein concentrations were measured in the left prefrontal cortex 24 h after blast expsoure using western blot analysis. A significant difference between groups was observed for PKCα. *Post-hoc* comparison between control and single blast (*p<0.05), and between single blast and single blast + bryostatin-1 (##p<0.01) (**a**). A significant difference between groups was observed for PKCδ. *Post-hoc* comparison between control and single blast (**p<0.01), and control and single blast + bryostatin-1 (*p<0.05) (**b**). A significant difference between groups was observed for PKCε. *Post-hoc* comparison between control and single blast (*p<0.05), and between control and single blast + bryostatin-1 (**p<0.01) (**c**). Bryostatin-1 significantly decreased PKCα levels and increased PKCε levels when administered after blast exposure

Author Manuscript Author Manuscript Author Manuscript Author Manuscript

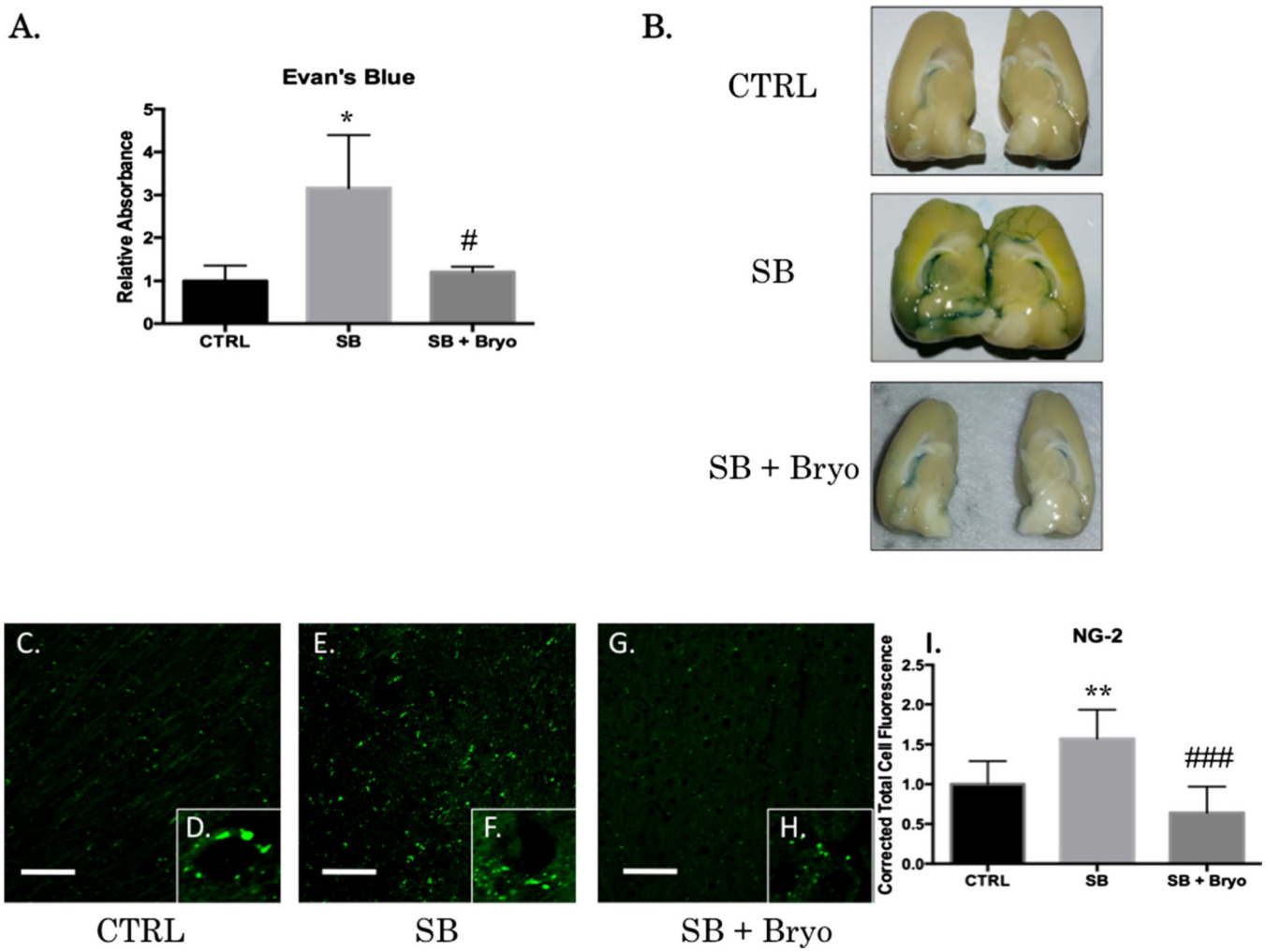

Fig. 4.

Bryostatin-1 preserves BBB integrity. Evan's blue binds to albumin and is a widely used marker for detecting breaches in the BBB. NG-2 is a proteoglycan found in pericytes that will be increased when the BBB is disrupted. Scale bar=100 μm in left prefrontal cortex. A significant difference between groups was observed for EB absorbance in the brain after femoral vein injection post-blast. *Post-hoc* comparison revealed a significant difference between control and single blast (*p<0.05), and between single blast and single blast + bryostatin-1 (#p<0.05) (**a**). Gross examination revealed increased EB staining in the left hemisphere following blast exposure that was decreased when bryostatin-1 was given following blast (**b**). A significant difference between groups was observed for NG-2 IHC fluorescent staining (**c–h**). *Post-hoc* comparison revealed a significant difference between control and single blast (**p<0.01), and between single blast and single blast + bryostatin-1 (###p<0.001) (**i**)

Author Manuscript Author Manuscript Author Manuscript Author Manuscript

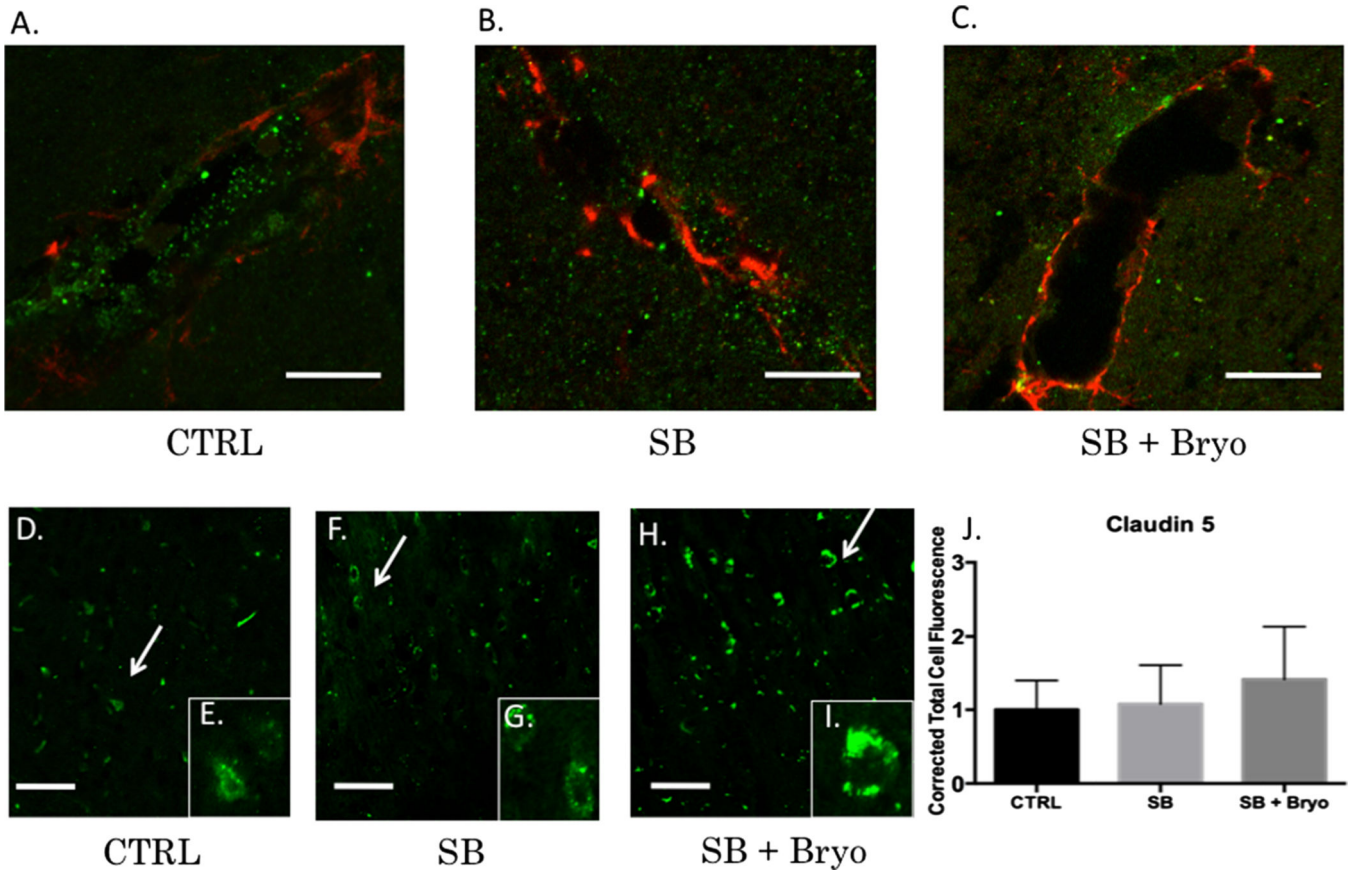

Fig. 5.

Vasculature disruption after blast exposure is independent of claudin-5 regulation. PKCα specifically regulates occludin, ZO-1, and VE-Cadherin, but not claudin-5. Claudin-5 levels may therefore be independent of bryostatin-1 modulation. Scale bar=5 μm in the left prefrontal cortex (**a–c**). Scale bar=100 μm in the left prefrontal cortex (**d–j**). VWF (*green*) was co-localized with GFAP (*red*) to give a visual representation of cerebral vasculature. Control vasculature in the left prefrontal cortex was visibly intact (**a**). Twenty-four hours after blast exposure left prefrontal cortex vasculature was visibly disrupted as indicated by the sparse VWF staining (**b**). Bryostatin-1 preserved vasculature integrity when administered after blast exposure (**c**). No significant differences were observed between groups for claudin-5 using fluorescent IHC (**d–j**)

Author Manuscript Author Manuscript Author Manuscript Author Manuscript

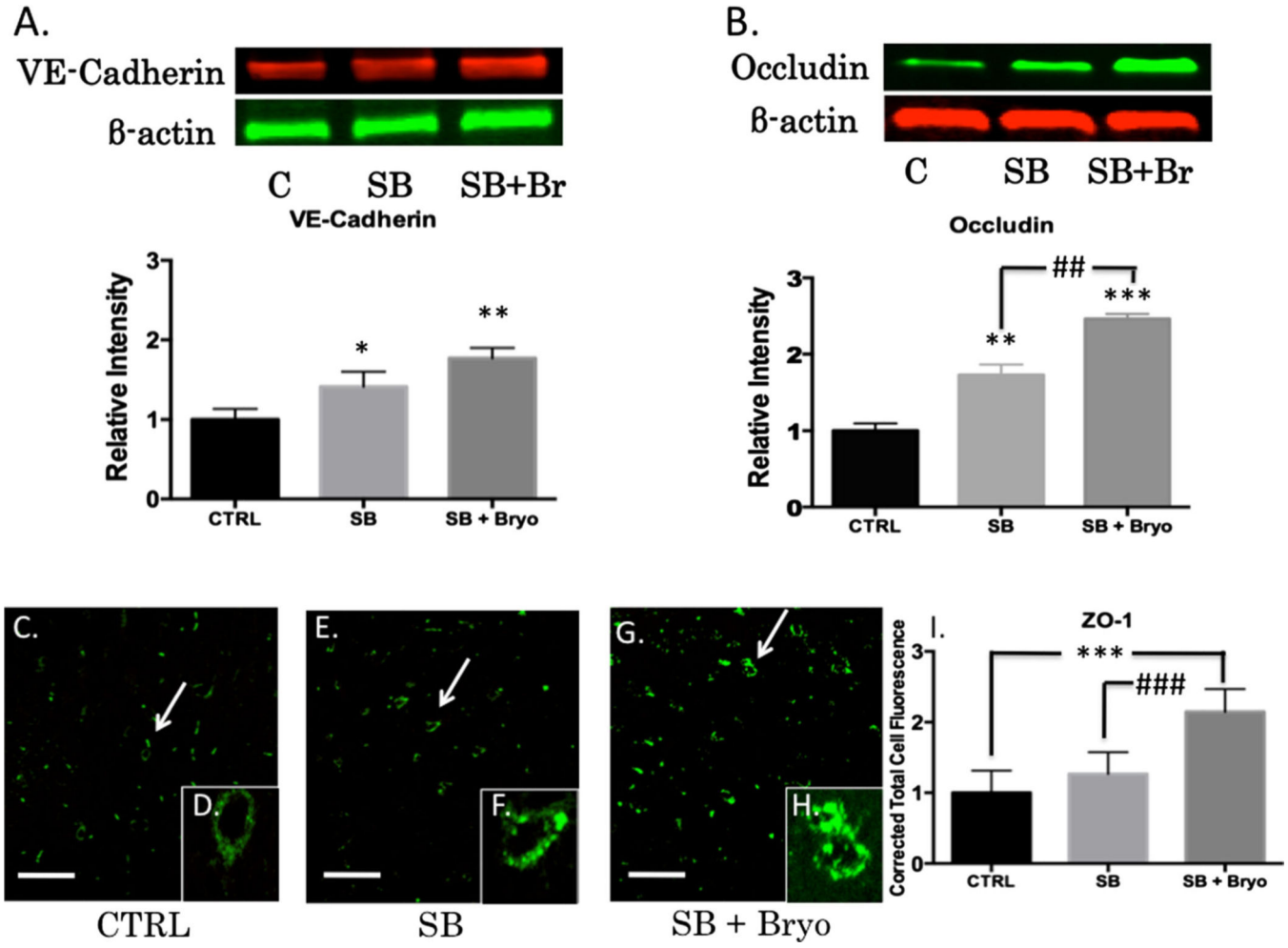

Fig. 6.

Bryostatin-1 significantly increases tight junction proteins. Our data show that bryostatin-1 significantly upregulated tight junction proteins leading to maintenance of BBB integrity following blast TBI. Scale bar=100 μm in left prefrontal cortex. A significant difference was observed between groups using western blot for VE-Cadherin with post hoc comparison showing significance between control and single blast (*p<0.05), and between control and single blast + bryostatin-1 (**p<0.01) 24 h after blast exposure (**a**). A significant difference was observed between groups using western blot for occludin with post hoc comparison showing significance between control and single blast (**p<0.01), between control and single blast + bryostatin-1 (***p<0.001), and between single blast and single blast + bryostatin-1 (##p<0.01) 24 h after blast exposure (**b**). A significant difference was observed between groups using fluorescent IHC for ZO-1 with post hoc comparison showing significance between control and single blast + bryostatin-1 (***p<0.001), and between single blast and single blast + bryostatin-1 (###p<0.001) 24 h after blast exposure (**c**)

Author Manuscript Author Manuscript Author Manuscript Author Manuscript

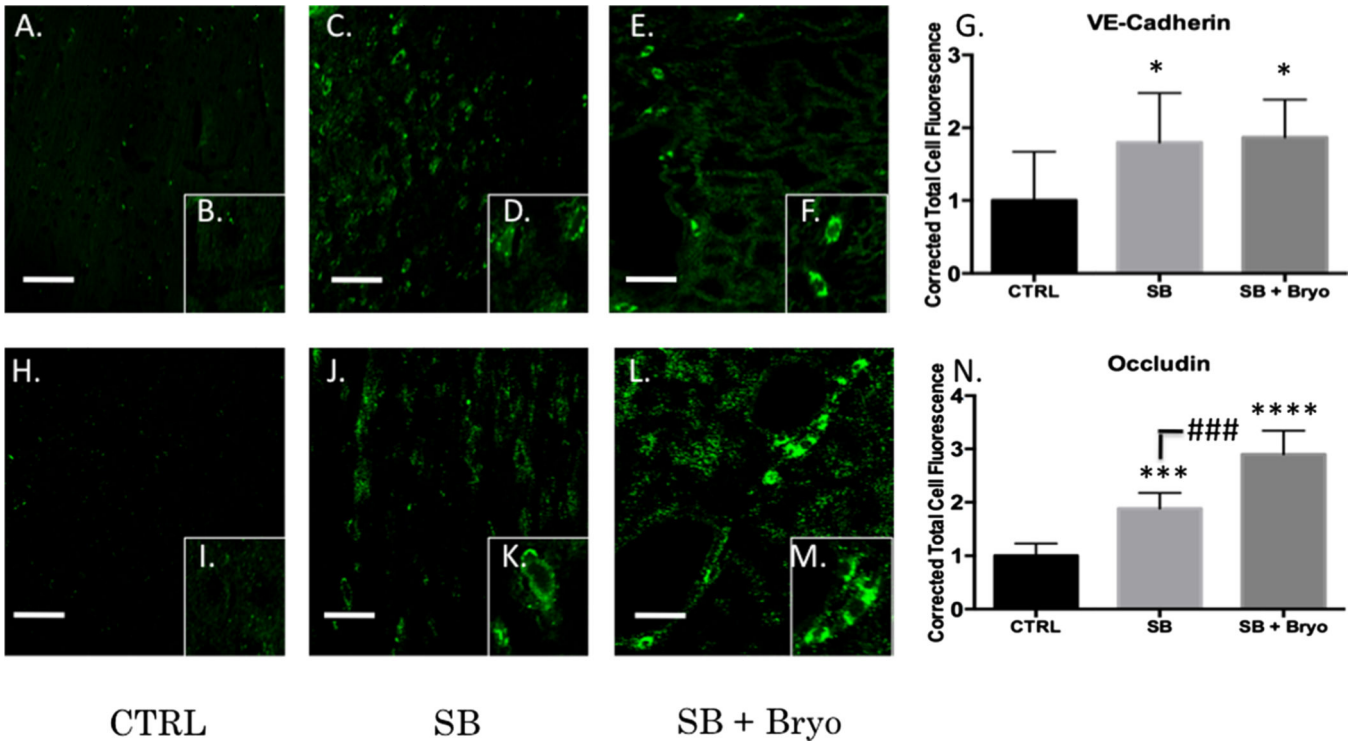

Fig. 7.

Tight junction protein expression was increased by bryostatin-1 at vasculature. Tight junction protein return of function is necessary for restoration of BBB integrity. Scale bar=75 μm in left prefrontal cortex. A significant difference was observed between groups using fluorescent IHC for VE-Cadherin with post hoc comparison showing significance between control and single blast (*p<0.05), and between control and single blast + bryostatin-1 (*p<0.05) 24 h after blast exposure (**a–g**). A significant difference was observed between groups using fluorescent IHC for occludin with *post-hoc* comparison showing significance between control and single blast (***p<0.001), between control and single blast + bryostatin-1 (****p<0.0001), and between single blast and single blast + bryostatin-1 (###p<0.001) 24 h after blast exposure (**h–n**)

Author Manuscript Author Manuscript Author Manuscript Author Manuscript

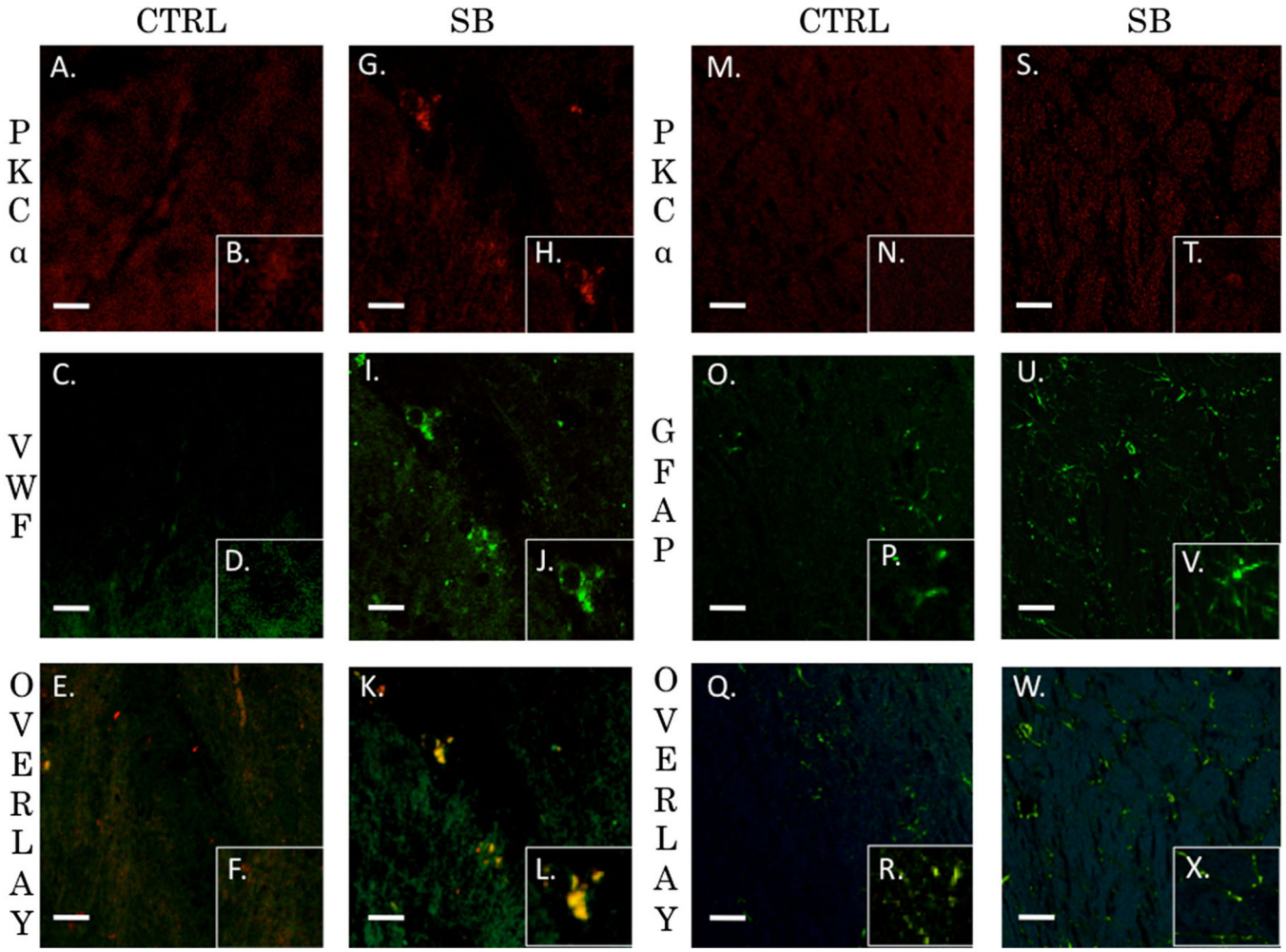

Fig. 8.

PKCα co-localized with endothelial cells but not astrocytes. Both astrocytes and endothelial cells are critical for maintenance of the BBB. PKCα activity within endothelial cells plays an intimate role in regulating extracellular tight junction proteins. Fluorescnt IHC red staining for PKCα, green staining for VWF (endothelial) or GFAP (astocyte), and yellow is overlay. Scale bar=20 μm in left prefrontal cortex. PKCα (**a**) with inlay (**b**) and VWF (**c**) with inlay (**d**) have a weak overlay with a Pearson's coefficient of r=0.395 seen in (**e**) with inlay (**f**) for control animals. PKCα (**g**) with inlay (**h**) and VWF (**i**) with inlay (**j**) have a very strong overlay with an overlap coefficient of r=0.954 seen in (**k**) with inlay (**l**) 24 h post blast exposure. PKCα (**m**) with inlay (**n**) and GFAP (**o**) with inlay (**p**) have a weak overlay with a Pearson's coefficient of r=0.351 seen in (**q**) with inlay (**r**) for control animals. PKCα (**s**) with inlay (**t**) and GFAP (**u**) with inlay (**v**) have a weak overlay with an overlap coefficient of r=0.379 seen in (**w**) with inlay (**x**) 24 h post blast exposure

Author Manuscript Author Manuscript Author Manuscript Author Manuscript

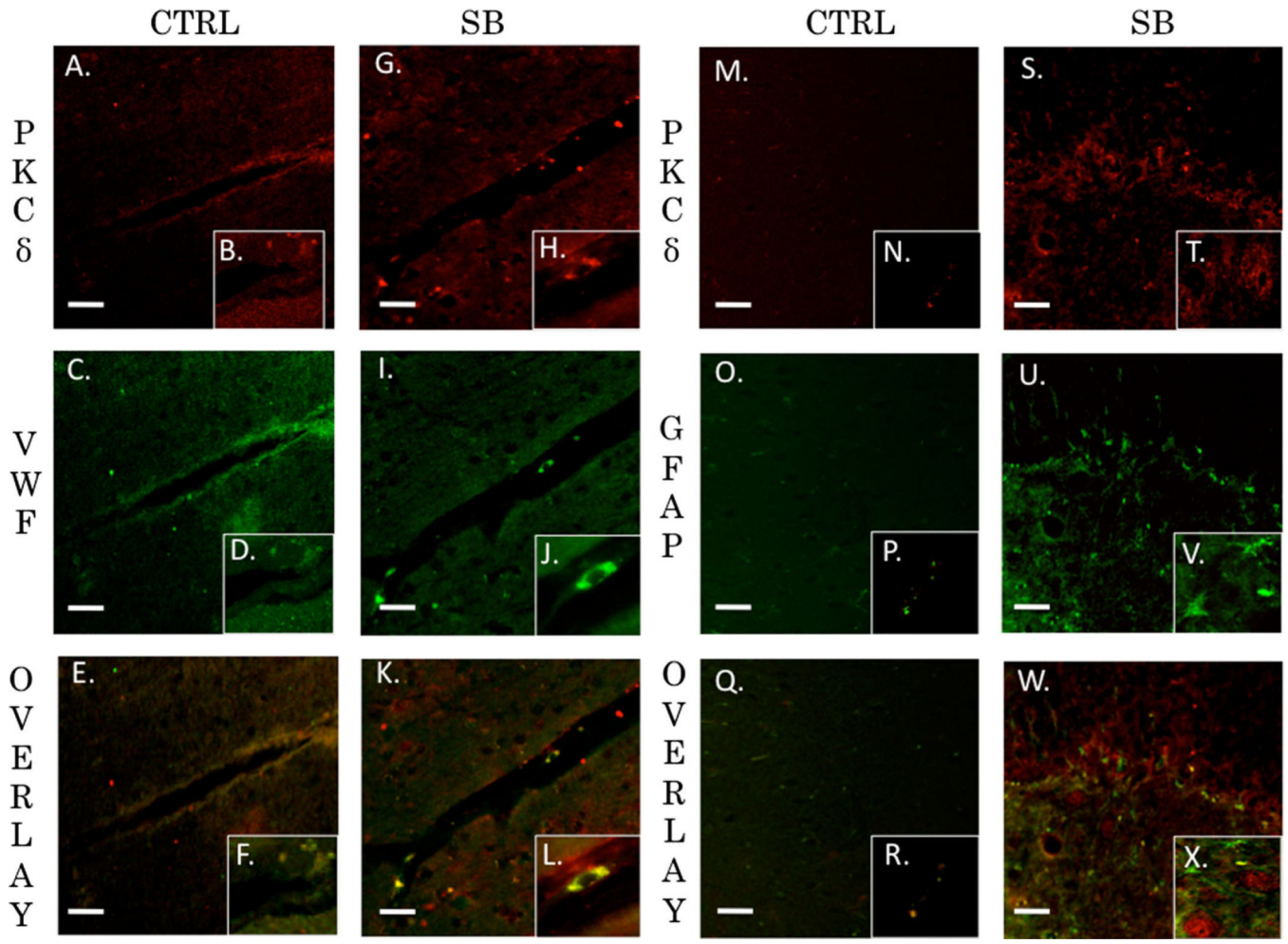

Fig. 9.

PKCδ co-localized with endothelial cells but not astrocytes. PKCδ plays an important role in mediating vascular tone. Its role in regulation of tight junction proteins is not completely understood. Fluorescent IHC red staining for PKCδ, green staining for VWF (endothelial) or GFAP (astocyte), and yellow is overlay. Scale bar=20 μm in left prefrontal cortex. PKCδ (**a**) with inlay (**b**) and VWF (**c**) with inlay (**d**) have a moderate overlay with a Pearson's coefficient of r=0.61 seen in (**e**) with inlay (**f**) for control animals. PKCδ (**g**) with inlay (**h**) and VWF (**i**) with inlay (**j**) have a strong overlay with an overlap coefficient of r=0.88 seen in (**k**) with inlay (**l**) 24 h post blast exposure. PKCδ (**m**) with inlay (**n**) and GFAP (**o**) with inlay (**p**) have a very weak overlay with a Pearson's coefficient of r=0.029 seen in (**q**) with inlay (**r**) for control animals. PKCδ (**s**) with inlay (**t**) and GFAP (**u**) with inlay (**v**) have a moderate overlay with an overlap coefficient of r=0.449 seen in (**w**) with inlay (**x**) 24 h post blast exposure

Author Manuscript Author Manuscript Author Manuscript Author Manuscript

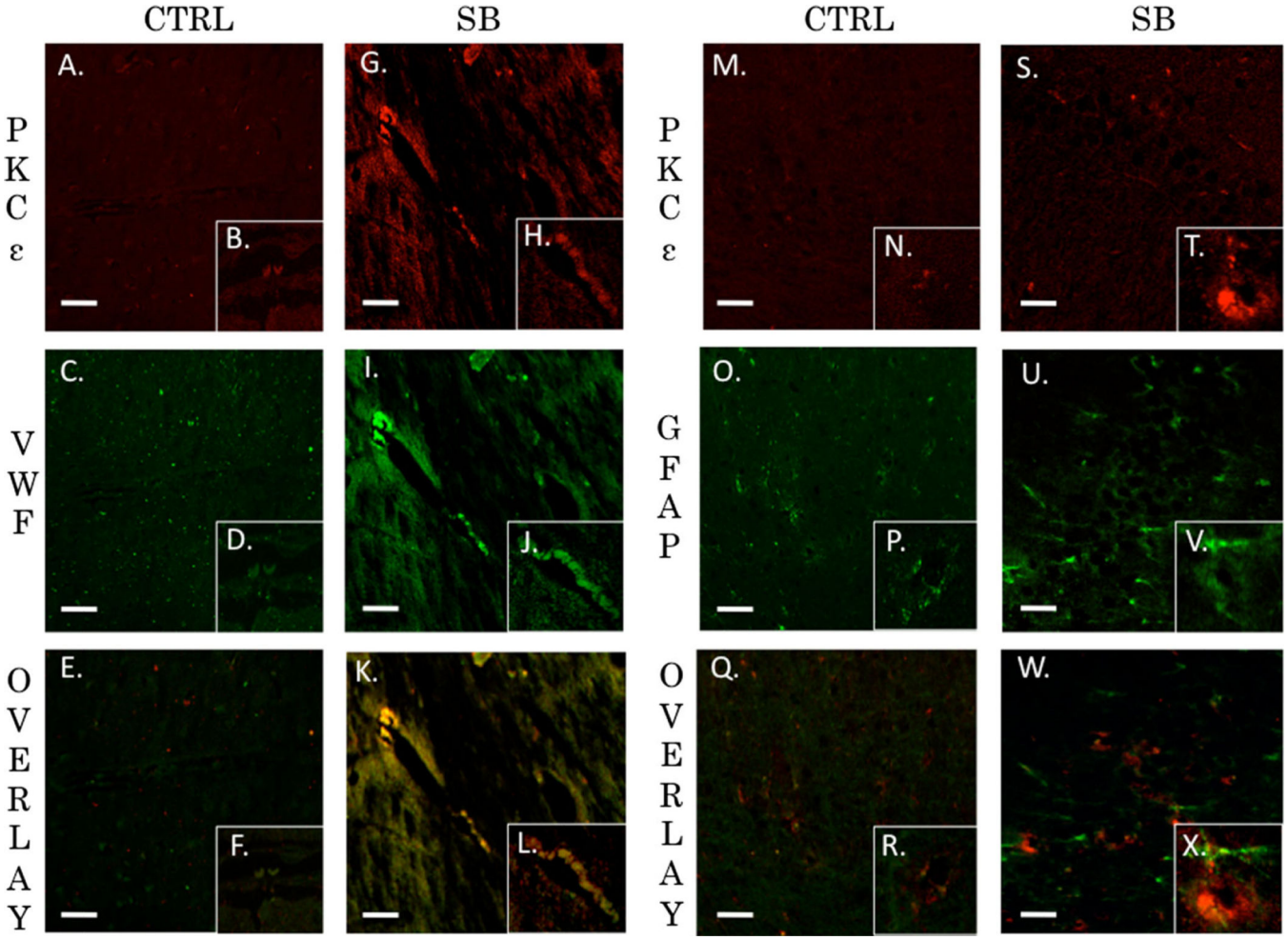

Fig. 10.

PKCε co-localized with endothelial cells but not astrocytes. PKCε contributes to neuroprotection when increased after brain injury. PKCε has been associated with improved cognitive performance and decreased neurodegeneration. Fluorescent IHC red staining for PKCε, green staining for VWF (endothelial) or GFAP (astocyte), and yellow is overlay. Scale bar=20 μm in left prefrontal cortex. PKCε (**a**) with inlay (**b**) and VWF (**c**) with inlay (**d**) have a very weak overlay with a Pearson's coefficient of r=0.004 seen in (**e**) with inlay (**f**) for control animals. PKCε (**g**) with inlay (**h**) and VWF (**i**) with inlay (**j**) have a strong overlay with an overlap coefficient of r=0.978 seen in (**k**) with inlay (**l**) 24 h post blast exposure. PKCε (**m**) with inlay (**n**) and GFAP (**o**) with inlay (**p**) have a weak overlay with a Pearson's coefficient of r=0.133 seen in (**q**) with inlay (**r**) for control animals. PKCε (**s**) with inlay (**t**) and GFAP (**u**) with inlay (**v**) have a weak overlay with an overlap coefficient of r=0.394 seen in (**w**) with inlay (**x**) 24 h post blast exposure